PROCEEDINGS OF SPIE ON CD

Third International Conference on Remote Sensing and Geoinformation of the Environmeny (RSCy2015)

16 - 19 March 2015
Paphos, Cyprus

Vol. 9535

SPIE.

GETTING STARTED

PROCEEDINGS OF SPIE ON CD

Acrobat Reader 5 or higher is required.

Acrobat Reader 9 or higher recommended.

Click here to download from Adobe's web site.

Setting Options

Before navigating the CD, please do the following:

For Acrobat versions 5-7: from the Edit menu, select Preferences>General; make sure that the option "Open Cross-Document Links in Same Window" is not selected.

For Acrobat versions 8 and 9: from the Edit menu, select Preferences>Documents; make sure that the option "Open Cross-Document Links in Same Window" is not selected.

SPIE.

COPYRIGHT

PROCEEDINGS OF SPIE ON CD

© Society of Photo-Optical Instrumentation Engineers (SPIE).

All rights reserved.

Single-User Edition

SPIE grants to users limited license to copy documents on this CD-ROM in print and/or electronic form for personal research or educational use. Articles may be downloaded, stored on a hard drive or other storage device, or printed in hard copy form, with the following restrictions and exceptions:

Systematic or multiple-copy reproduction or republication, electronic retransmission to another location, print or electronic duplication of any material on the CD-ROM for a fee or for commercial purposes, or altering or recompiling any contents of the CD-ROM are not permitted.

By choosing to view, download, or print any portion of this material, you agree to all the provisions of the copyright law protecting it and to the terms and conditions established by the copyright holder.

Inquiries or comments regarding copyright should be directed to the SPIE Director of Publications.

SPIE.

CONTENTS

PROCEEDINGS OF SPIE ON CD

Volume 9535: Third International Conference on Remote Sensing and Geoinformation of the Environment (RSCy2015)

Volume 9535: Third International Conference on Remote Sensing and Geoinformation of the Environment (RSCy2015)

Editors: Diofantos G. Hadjimitsis, Kyriacos Themistocleous, Silas Michaelides, Giorgos Papadavid

Drought in Nicosia using Standardized Precipitation Index SPI-n and BMDI drought index [9535-83]
M. Theophilou, D. Serghides

REMOTE SENSING, SAR AND RADAR, ENVIRONMENT

Forest canopy height estimation using double-frequency repeat pass interferometry [9535-33]
K. Karamvasis, V. Karathanassi

DSM generation from Sentinel and COSMO-SkyMed data using interferometry and radargrammetry: a case study from Mykonos, Greece [9535-71]
K. Nikolakopoulos, A. Kyriou, V. Charalampopoulou

Exploitation of satellite optical and SAR data for public work studies [9535-63]
C. Ioannidis, S. Soile, A. Stamos, D. Vassilaki, E. Maltezos, S. Verykokou

Automated motion detection from space in sea surveilliance [9535-68]
E. Charalambous, J. Takaku, P. Michalis, I. Dowman, V. Charalampopoulou

Development of a rule-based algorithm for rice cultivation mapping using Landsat 8 time series [9535-57]
C. Karydas, P. Toukiloglou, C. Minakou, I. Gitas

Web-GIS platform for green infrastructure in Bucharest, Romania [9535-45]
M. Sercaianu, F. Petrescu, M. Aldea, L. Oana, G. Rotaru

Quantitative correlation of rainfall and earth surface displacements for slope stability studies [9535-60]
C. Steiakakis, Z. Agioutantis, E. Apostolou, G. Papavgeri, A. Tripolitsiotis

LIDAR

Lidar detection of carbon dioxide in volcanic plumes [9535-50]
L. Fiorani, S. Santoro, S. Parracino, G. Maio, M. Del Franco, A. Aiuppa

Effect of enhanced x-ray flux on the ionosphere over Cyprus during solar flares [9535-55]
M. Mostafa, H. Haralambous

REMOTE SENSING

Interpolation and elevation errors: the impact of the DEM resolution [9535-43]
G. Achilleos

Geometric registration of remotely sensed data with SAMIR [9535-8]
M. Gianinetto, L. Barazzetti, L. Dini, A. Fusiello, R. Toldo

Context-awareness in ubiquitous computing and the mobile devices [9535-11]
N. Akçit, E. Tomur, M. Karslıoğlu

Monitoring asphalt pavement damages using remote sensing techniques [9535-82]
C. Mettas, K. Themistocleous, K. Neocleous, A. Christofe, K. Pilakoutas, D. Hadjimitsis

WORKSHOP - CULTURAL HERITAGE

Feature enhancement from electrical resistivity data in an archaeological survey: the Sapelos hillfort experiment (Boticas, Portugal) [9535-29]
M. Alves, P. Bernardes, L. Fontes, M. Martins, J. Madeira

A Polish perspective on optical satellite data and methods for archaeological sites prospection [9535-73]
D. Ruciński, W. Rączkowski, J. Niedzielko

Searching for hidden houses: optical satellite imagery in archaeological prospection of the early Neolithic settlements in the Kujawy region, Poland [9535-77]
W. Rączkowski, D. Rucinski

Romantic versus scientific perspective: the ruins of Radlin palace in Wielkopolska region in the light of remote sensing techniques [9535-76]

A. Wilgocka, D. Ruciński, W. Rączkowski

Assessing the damage of Chelmo Mount, Poland: a remote sensing perspective analyzing and interpreting ALS and satellite data [9535-74]

M. Kostyrko, D. Ruciński

Impact of modern evolution of Paphos town to its ancient necropoleis: a multi-temporal GIS and earth observation analysis [9535-21]

V. Lysandrou, A. Agapiou, D. Hadjimitsis

Mapping of traditional settlements by unmanned airborne vehicles towards architectural restoration [9535-86]

P. Partsinevelos, N. Skoutelis, A. Tripolitsiotis, S. Tsatsarounos, A. Tsitonaki, P. Zervos

The methodology of documenting cultural heritage sites using photogrammetry, UAV, and 3D printing techniques: the case study of Asinou Church in Cyprus [9535-79]

K. Themistocleous, M. Ioannides, A. Agapiou, D. Hadjimitsis

GIS - GEOLOGY

Marine spatial planning in Cyprus [9535-80]

D. Hadjimitsis, A. Agapiou, C. Mettas, K. Themistocleous, E. Evagorou, B. Cuca, C. Papoutsa, A. Nisantzi, R. Mamouri, G. Soulis, Z. Xagoraris, V. Lysandrou, K. Aliouris, N. Ioannou, G. Pavlogeorgatos

Tasselled Cap transform for change detection in the drylands: findings for SPOT and Landsat satellites with FOSS tools [9535-36]

A. Zanchetta, G. Bitelli, A. Karnieli

Analyzing green/open space accessibility by using GIS: case study of northern Cyprus cities [9535-20]

C. Kara, N. Akçit

Traffic accident analysis using GIS: a case study of Kyrenia City [9535-12]

C. Kara, N. Akçit

NATURAL HAZARDS

Burn severity estimation using GeoEye imagery, object-based image analysis (OBIA), and Composite Burn Index (CBI) measurements [9535-56]

E. Dragozi, I. Gitas, D. Stavrakoudis, C. Minakou

Subsidence mapping, characterization, and modeling: the ESA-GMES Terrafirma services [9535-3]

F. Raspini, S. Bianchini, C. Del Ventisette, S. Moretti, C. Loupasakis, D. Rozos, J. Duro, M. Garcia

PREFER: a European service providing forest fire management support products [9535-70]

G. Eftychidis, G. Laneve, F. Ferrucci, A. Sebastian Lopez, L. Lourenco, S. Clandillon, L. Tampellini, B. Hirn, D. Diagourtas, G. Leventakis

NATURAL HAZARDS - WATER SCIENCES

Rockfall risk evaluation using geotechnical survey, remote sensing data, and GIS: a case study from western Greece [9535-67]

K. Nikolakopoulos, N. Depountis, N. Vagenas, K. Kavoura, E. Vlaxaki, G. Kelasidis, N. Sabatakakis

Detection of small-scale rockfall incidents using their seismic signature [9535-35]

A. Tripolitsiotis, A. Daskalakis, S. Mertikas, D. Hristopulos, Z. Agioutantis, P. Partsinevelos

Modified-Fibonacci-Dual-Lucas method for earthquake prediction [9535-46]

A. Boucouvalas, M. Gkasios, N. Tselikas, G. Drakatos

POSTER SESSION: LAND COVER

Towards an unitary technical approach for monitoring urban growth in Romania using remote sensing data [9535-53]

M. Aldea, F. Petrescu, M. Sercaianu, F. Gaman, C. Iacoboaea

POSTER SESSION: LIDAR

LIDAR and airphoto technology in the study of the Black Sea accumulative coasts [9535-32]

E. Boyko, V. Krylenko, M. Krylenko

POSTER SESSION: NATURAL HAZARDS

Multi-temporal change image inference towards false alarms reduction for an operational photogrammetric rockfall detection system [9535-85]

P. Partsinevelos, C. Kallimani, A. Tripolitsiotis

POSTER SESSION: NEURAL NETWORKS

Developing an ANN electron density profile model over Cyprus based on ionosonde measurements [9535-59]

H. Haralambous, H. Papadopoulos, M. Mostafa

POSTER SESSION: REMOTE SENSING

Cross validation of geotechnical and geophysical site characterization methods: near surface data from selected accelerometric stations in Crete (Greece) [9535-42]

C. Loupasakis, P. Tsangaratos, D. Rozos, T. Rondoyianni, A. Vafidis, G. Kritikakis, M. Steiakakis, Z. Agioutantis, A. Savvaidis, P. Soupios, I. Papadopoulos, N. Papadopoulos, A. Sarris, M. Mangriotis, U. Dikmen

A sensitivity study for the calibration of hyperspectral spectrometer on board the geostationary multipurpose satellite of Korea [9535-25]

M. Ahn, M. Kang, X. Liu, J. Kim

Estimation of uncertainties in the spectral response function of the water vapor channel of a meteorological imager [9535-22]

M. Ahn, S. Lee, D. Kim

POSTER SESSION: WATER SCIENCES

Delineating sea surface water quality regions from remotely sensed data using textural information [9535-28]

P. Kyriakidis, G. Vasios, D. Kitsiou

Mapping the Anapa bay bar geosystems on the basis of satellite remote sensing and ground data [9535-66]

V. Kravtsova, O. Tutubalina, V. Krylenko, M. Krylenko, E. Chalova

Feature enhancement from electrical resistivity data in an archaeological survey: the Sapelos hillfort experiment (Boticas, Portugal).

Mafalda Alves[*a], Paulo Bernardes [a], Luís Fontes [a], Manuela Martins [a] and Joaquim Madeira [b]
[a] University of Minho – Unit of Archaeology, Av. Central, Ed. Congregados, n.º 100, 4710-229 Braga, Portugal; [b] University of Aveiro – DETI/IEETA, Campus Universitário de Santiago, 3810-193 Aveiro, Portugal

ABSTRACT

The PoPaTERVA project is developing applied research regarding the comprehension of the multi-layered cultural background of the Terva Valley Archaeological Park, in Boticas, Portugal. One of the main aspects focused on the project is the appliance of remote sensing techniques to enhance non visible archaeological features. An earth resistance tomography (ERT) survey was carried out at the Sapelos hillfort, by the specialized SINERGEO geophysicist's team, using a Wenner-Schlumberger array. The resulting data was analyzed by the authors in order to extract and verify valid archaeological features regarding the settlement's structures. There are several adequate systems that can be used to visualize the surveyed data (x, y, z, Ω). However, the authors preferred the open source Visualization Toolkit (VTK) from Kitware Inc., since it supports several visualization and modelling techniques that are useful for interpretation purposes in archaeological contexts: for instance, it is possible to represent the archaeological site as a virtual scale model, which can be freely manipulated. For the Sapelos hillfort, two distinct visualizations were developed to represent the acquired electrical resistivity data. The first one is used to create a comprehensive volume from the surveyed data, which is imported as structured 3D points and mapped into a 3D volume. However, this representation does not provide the necessary insight for analysis purposes, so a second visualization is needed to cluster the relevant data for archaeological research. This visualization is based on contouring algorithms that generate isosurfaces from scalar resistivity values (Ω), therefore enhancing the features with potential archaeological interest.

Keywords: Archaeological Geophysics, Electrical Resistivity, Resistivity Imaging, VTK.

1. INTRODUCTION

Geophysical methods are widely used in Archaeology since the second half of the twentieth century[1,2]. The most common are ground penetrating radar (GPR), magnetic and electromagnetic surveys and earth resistance tomography (ERT)[3,4]. Having in mind the particular geological background of the Sapelos hillfort, the first geophysical approach prepared was an ERT survey.

The primary goal of this case study was to evaluate the results of an ERT survey regarding the detection of non-visible archaeological features. The survey was conducted at the site as part of a much broader investigation regarding the historical landscape patterns in the Terva Valley Archaeological Park – PAVT – area. This research is being conducted under an umbrella project, referred to as the PoPaTERVA 2013-2016. The research program, led by the Unit of Archaeology of the University of Minho, focuses on distinct layers of the landscape structure and the investigation is taking place in cross-platform projects, concerning Archaeology, Paleoenvironments, Geophysics, Geo-Thermal Hydrology, Biology and Tourism[5].

The next section will shortly describe the well-known geological and historical background that support this project and which contextualize the surveyed area. The third section explains the geological survey methodology that was used in this area for archaeological research purposes. The survey was contracted to an external Geology company (SINERGEO), led by Bruno Pereira[6]. The raw data obtained was practically indecipherable for non-experts, therefore there was the need for a visual enhancement and clustering of the data, so that the anomalies which might relate to archaeological features could be analysed in a more efficient way.

*mafaldasda@gmail.com; phone +351 253 601 270.

Third International Conference on Remote Sensing and Geoinformation of the Environment (RSCy2015), edited by Diofantos G. Hadjimitsis, Kyriacos Themistocleous, Silas Michaelides, Giorgos Papadavid,
Proc. of SPIE Vol. 9535, 95350T · © 2015 SPIE · CCC code: 0277-786X/15/$18 · doi: 10.1117/12.2192568

For that purpose, the Visualization Toolkit (VTK) from Kitware Inc. was used since, on one hand, it is an open-source package and freely available as a C++ class library for 3D computer graphics, image processing and visualization; on the other hand, VTK supports a great variety of visualization algorithms and advanced modelling techniques that can be used to increase the understanding of the surveyed data[7]. The complete visualization procedure of the surveyed data is explained in the fourth section.

In the last sections the authors present the results from this case study as well as some conclusions and directives for future work.

2. SITE CONTEXT

2.1 Geological background

The Terva valley is located in the European Variscan Belt, more specifically in the paleogeographical area of the Iberian Peninsula referred to as the Galicia-Trás-os-Montes Zone[8] (Figure 1A, 1B). The valley holds a lithological formation that outcomes from the late Hercinic orogenic movements, resulting, in this particular area, into the metasedimentary units of the Para-autochthenon, dating back to the Silurian[9]. Due to a lesser thickening of the crustal nappe[10], there exists particularly in the Terva Valley, a type of two-mica alcaline granite, locally known as *Granito de Chaves*[11] (Figure 1C). Resulting from Variscan collisional magmatism, this granite's metallogenetic composition often bears important mineralizations, such as W, Sn, Au or Li[8].

The Sapelos settlement stands over a levelled hill top, crossed by quartz veins, which ridge trough the surface, following the general orientation of NNE-SSW, trending with the Régua-Verin tectonic fault[11]. The soils are composed by granitic based deposits, slightly thick, containing altered granitic sands, mixed with quartz stones and boulders that fractured from the existing veins[6]. The quartz veins have formed in layered *Pinch and Swell* structures, varying in thickness from meters to centimetres[6].

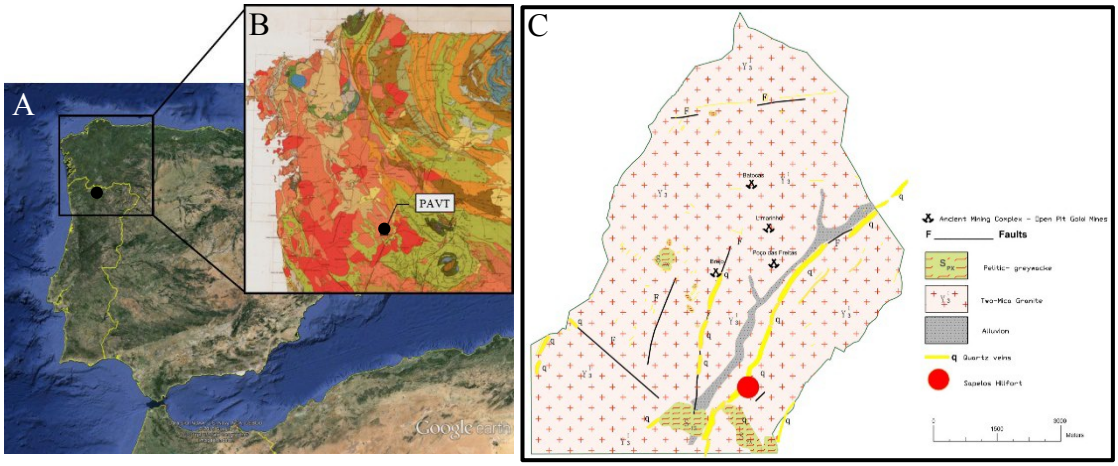

Figure 1. (A) General localization of the Terva Valley Archaeological Park – PAVT. (B) The PAVT area in the NW Iberia Geological Map 1:500 000[12]. (C) PAVT simplified geological map, based on the Geological Map of Portugal, 1: 200 000[13].

2.2 Historical background

The Sapelos hillfort is one of the nine fortified settlements occupied during Iron Age in the upper Terva River valley (Figure 2A). The number of known sites, rather high if we attend to the regional context for the same period, is, in our opinion, directly related with exploitation of the metallic mineral resources available, namely gold and tin, which later on attracted the Romans into developing large and extensive open pit mines along the valley's mineral cores.

Understanding the Sapelos hillfort´s chronological path is a fundamental aspect for the comprehension of the valley's historical construction process, as this is one of its most preeminent landscape bastions. This hillfort strategically controls the entire valley from its southern limit, standing in a privileged position towards the natural crossing routes and the mineral cores. The hillforts's surface has micro-topographical aspects that induce the localization of buried structures

and some remaining walls are partially visible amongst the vegetation cover (Figure 2B). The settlement is heavily fortified by three meters wide defensive walls, displayed over two distinct lines around the hill top and slopes (Figure 2D). The Sapelos hillfort also bears a singular landscape architectural module, unique to its surroundings: it has a complex system of deep trenches, one of which surrounding the entire hill and seven other arranged in a deltoid figure towards the valley. Sometimes referred to as mining trenches, the fact that the Sapelos quartz veins have no occurrence of metallic minerals is more coherent with the hypothesis that these are, in fact, negative structures for defensive purposes.

Standing before a heavily fortified settlement, so far with no material evidences of occupation beyond the general timescale for the NW Iberia's Iron Age, raised the need for understanding the time and the reasons behind those complex fortification structures.

At present, a team of archaeologists is conducting trial archaeological trenches at Sapelos hillfort, assessed by the ERT results (Figure 2B, 2C, 2D). This research, related to the PoPaTERVA 2013-2016 project, integrates a broader investigation program over the Iron Age landscape in the PAVT area.

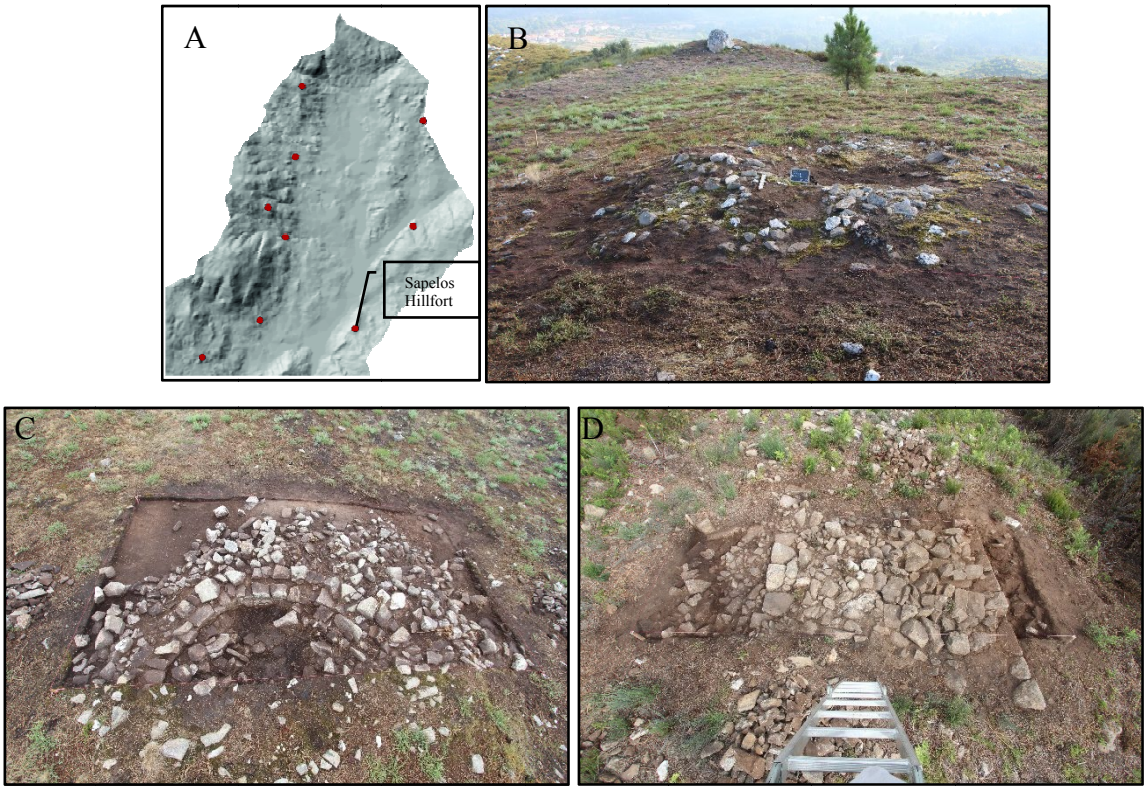

Figure 2. (A) Iron Age fortified settlements in the PAVT area. (B) The hillfort's top platform: aspect of a micro-topographical anomaly after vegetation clearing. (C) Archaeological trench over the same anomaly revealed the existence of a circular building. (D) Archaeological trench over a part of the defensive wall.

3. SURVEY METHODOLOGY

3.1 ERT Specifications

The ERT was done over a linear grid with an *X* parallel offset distance of 4 m, crossed by *Y* distal lines with 10 m spacing (Figure 3). For this survey, the team used a SYSCAL R1 Plus from IRIS Instruments and a total of 72 electrodes for an inter-electrode linear spacing of 1m [6].

Figure 3. ERT survey grid established for the Sapelos hillfort.

For this survey the method used was the Wenner-Schlumberger array. The data was processed with *RES2INV*®, using the software's smoothness-constrained least-squares method[14], based on the following equation[15,6,14]:

$$(J^T J + 1F)\Delta q_k = J^T g - 1F q_k \tag{1}$$

where

$$F = \alpha_X C_X^T C_X + \alpha_Z C_Z^T C_Z \tag{2}$$

$$C_X = \text{horizontal roughness filters} \tag{3}$$

$$C_Z = \text{vertical roughness filters} \tag{4}$$

$$J = \text{Jacobian matrix of partial derivatives} \tag{5}$$

$$1 = \text{damping factor} \tag{6}$$

$$q = \text{model change vector} \tag{7}$$

$$g = \text{data misfit vector} \tag{8}$$

The inter-electrode arrange started to return data at ~0.50 m depth below current surface. The resulting data had an Ohm (Ω) class range between 1.586.377,75 Ω and 146,03 Ω.

3.2 First Data Analysis

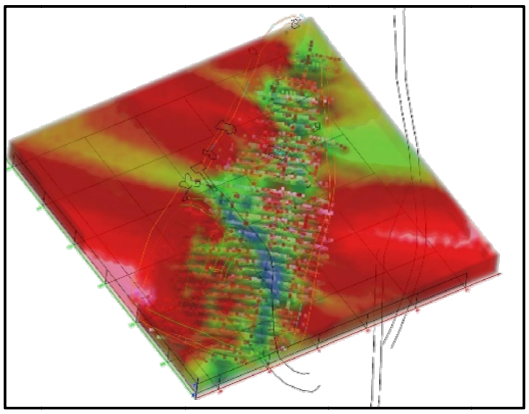

Figure 4. Isovolume interpolation, rendered with the individual sections. The model is overlapped by the main features from the site's topographical survey[6]. (Courtesy of SINERGEO)

The first visualization (Figure 4) of the data revealed very high resistivity values, directly related to the quartz veins existing at the site. This generated visual noise that masked the detection of close ranged anomalies most generally related to archaeological features. Pursuing the objective of minimizing noise, the data was sorted by relating the resistivity points with the physical evidences, triggering the detection of cluster patterns. In that way, it was possible to reduce the quartz interference, by intersecting the Ω values obtained in points where parts of remaining building walls were visible and with some vertical presence expected. Resulting from this cross-checking, the class range was focused between 24.000 Ω and 45000 Ω. This decision implies losing information as it significantly reduces the data scope. Assuming this, the results gathered were frankly positive, regarding the detection of anomalies, and they will be discussed in detail in the fifth section.

4. DATA VISUALIZATION

For the Sapelos' data, the authors used two different, but complementary, visualization procedures to represent the acquired electrical resistivity data. The first approach is a more general, volumetric based representation of the surveyed data, while the second clusters the significant data for archaeological research.

4.1 Volume-based data visualization

The surveyed data is integrated into a topological and geometrical regular array of 3D points. This geometric structure is is imported into the renderer (*vtkRenderer*) using a *vtkStructuredPointsReader* (a VTK source object). The reader output is a single *vtkStructuredPoints* data object that is mapped into a *vtkVolume* using the *vtkVolumeTextureMapper3D*. To enhance the volume representation it is indispensable to classify the relevant objects of interest within a specific dataset. In the current example the objects of interest are the settlement's structures. Consequently, to distinguish potential structures within the volume representation the transfer function in *vtkVolumeProperty* was defined taking into account the resistivity values set between 24.000 Ω and 45.000 Ω. The *vtkVolumeProperty* is an object where the properties, such as color and opacity associated to the volume rendering, are defined.

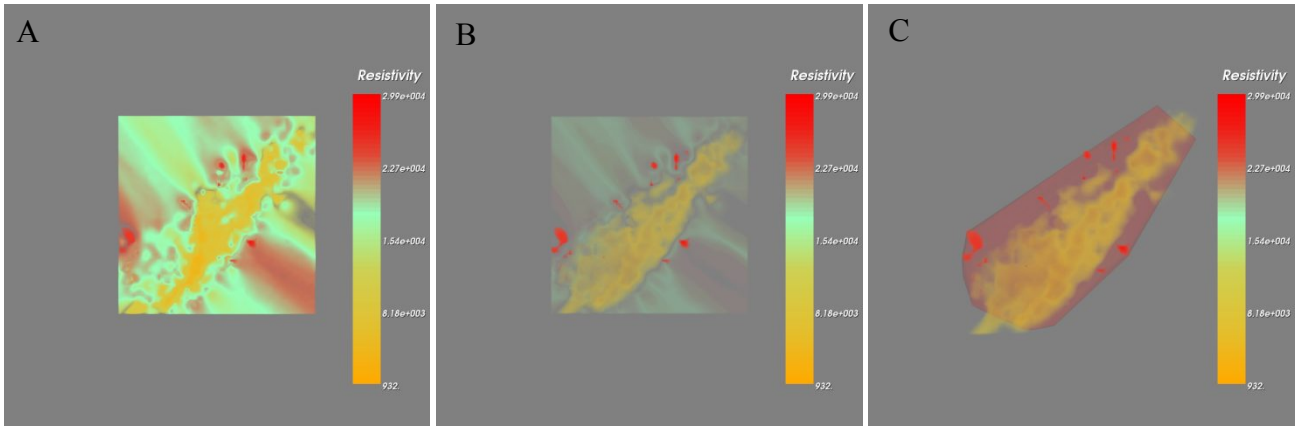

Figure 5. (A) Volumetric representation of the surveyed data. (B) Visual enhancement of the same representation. (C) Well-defined volume of interest.

The first volume rendering (Figure 5A) might be considered confusing for non-experts, since it is difficult to capture the exact volume of interest (VOI). But, by observing the scale bar in the figure it is easy to recognize that the VOI has resistivity values lower than 8.180 Ω and greater than 22.700 Ω. Therefore, to minimize the visual representation outside the VOI, the opacity values of the transfer function for the resistivity values between 8.180 Ω and 22.700 Ω have to be redefined. Figure 5B illustrates high opacity values (set to 100%) for resistivity higher than 22.700 Ω (potential structures), low values (set to 20%) for resistivity lower than 8.180 Ω (material inside the VOI), and extremely low values (set to 1%) for resistivity that ranges between 8.180 Ω and 22.700 Ω (outside the VOI). This visual representation is more defined than the first one; however it is still possible to enhance the delimitation of the VOI.

To create a better-defined VOI it is necessary to generate a bounding volume, using a 3D Delaunay filter. The structured 3D points are filtered by *vtkThresholdPoints* to extract the 3D points and store them as polygonal data. The threshold

criterion of *vtkThresholdPoints* is set coherently with the relevant objects of interest and the 3D Delaunay filter (*vtkDelaunay3D*) is applied to the resulting polygonal data to generate a surrounding 3D mesh (*vtkUnstructuredGrid*) that improves the perception of the data. The created mesh is mapped into a geometric entity (*vtkActor*) and added to the renderer. However, this mesh needs to have some degree of transparency to not obstruct the analysis of the data. Since *vtkActor* is a geometric object, the primary properties are set with *vtkProperty* that handles the color, the opacity and the representation of the object (surface, wireframe or points). In this specific case the opacity is set to 10% (Figure 5C).

4.2 Geometry extraction

Although the volumetric representation of the data already enabled a satisfactory understanding of the surveyed data, it does not provide the necessary insight for analysis purposes. Therefore, the visual accuracy has to be improved by clustering the surveyed data according to the resistivity values of interest. A contouring methodology was used to create the isosurfaces that represent probable objects of interest with resistivity values that range between 24.000 Ω and 45.000 Ω. Since the data are imported as structured 3D points, the *vtkMarchingContourFilter* object was used to generate the isosurfaces from the resistivity values (scalars). The surface normals of the resulting mesh are recomputed with the *vkPolyDataNormals* filter to improve mesh rendering. The output of this filter is mapped into a geometry object (*vtkActor*) and added to the renderer (Figure 6).

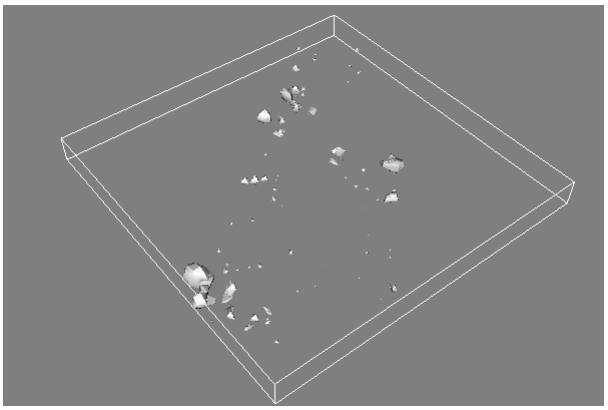

Figure 6. Isosurfaces of the clustered anomalies

4.3 Integration of the two visualizations

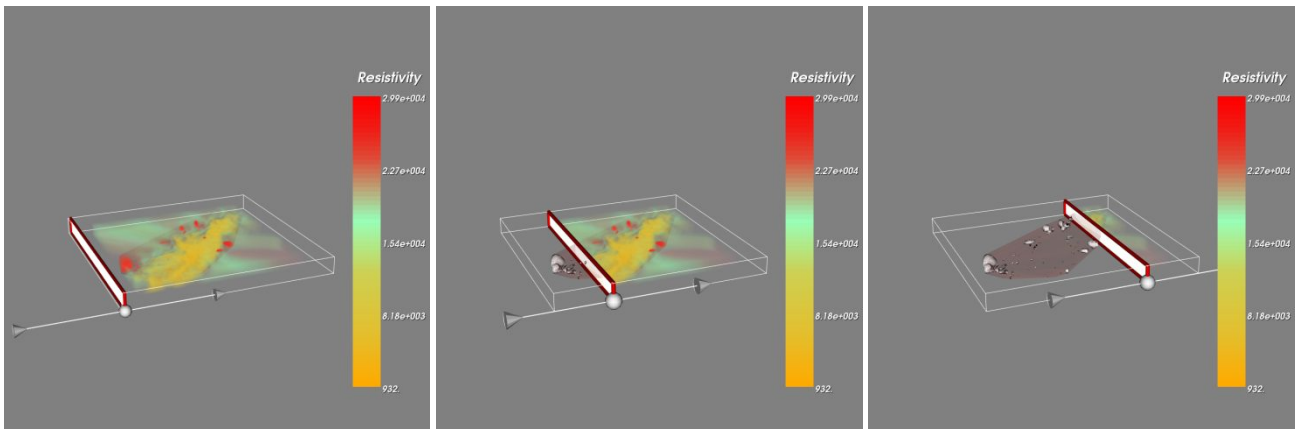

Figure 7. Interactive sweeping plane

These two visualizations can be combined and used to filter noise of the overall representation of the surveyed data, allowing a cleaner visualization of the objects of interest. But it is not enough to combine the two visualizations: it is necessary to create an interactive sweeping plane for dragging along an axis to separate the potential structures.

The implementation of interactive objects using VTK is usually performed with widgets that provide an interface to a complex operation. To implement the interactive sweeping plane a *vtkImplicitPlaneWidget* object is used. This 3D widget defines an infinite plane that is placed in the scene and is represented by a plane with a normal vector. This normal vector can be selected and moved to freely rotate the plane, while the plane itself can be translated in any direction. Figure 7 shows the implemented interactive sweeping plane that is immediately updated as the planes moves along the sweeping axis. To achieve the desired "cleaning" effect, it is also necessary to define a plane (*vtkPlane*) that is used as clipping plane: on one side of the plane the user observes the volume rendering on the other side the mesh from the contouring procedure. This plane is shared with the interaction handler (*vtkInteractionHandler*) and when the implicit plane widget is moved the user notices the "cleaning" of the noise preventing a clearer representation of the potential structures of interest.

5. DISCUSSION OF THE RESULTS AND CONCLUSIONS

First, the raw results from the survey were represented as an extremely compact data volume. To gain insight through the entire data came to be impossible, as the structures of interest were veiled by the quartz constraints.

Cross-checking the data by intersecting both resistivity and archaeological dimensions resulted in the successful mapping of several volumes of interest that are, in the authors' opinion, related to the archaeological subset of the hillfort. However, this relation is not always strictly obvious, as it also depends on the spacing between the electrical probes.

In Figure 8, one can observe a planar representation where the VOI are overlapped by the topographical points regarding the archaeological features visible on the ground. The signalled case (1) regards the building shown in Figure 2B and 2C. In this case, there is no VOI matching this particular building. From the archaeological excavation it is now known that this particular structure has no vertical expression at the depth of the first electrical signal (ca. 0,50 m). Thus, for future ERT surveys, reducing the inter-electrode spacing will be most certainly required.

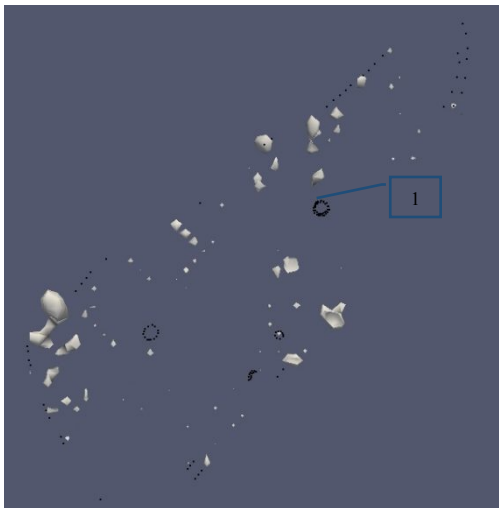

Figure 8. Superposition of the recognized archaeological features (represented with the black points) with the volumes of interest (represented as a grey mesh models).

Nevertheless, the visual results seem to make sense from an archaeological point of view, as the volumes of interest shown seem to indicate what appears to be the top defensive wall of the hillfort. In the same way, most of the smaller volumes of the inner area seem to indicate the presence of buried buildings associated with the settlement's occupation.

Working data from ERT surveys in order to evaluate non visible archaeological features is not, in any way, linear nor simple, mostly since there are a number of variables particular to each site that can substantially alter the electrical response to the features.

The Sapelos' experiment revealed that the usage of geophysical data processed with 3D visualization methods can be a powerful tool to enhance the analysis of the volumetric data and help an archaeological analysis for a given site.

ACKNOWLEDGMENTS

We would like to express our thanks to the SINERGEO's team (Bruno Pereira, João Azevedo, Jorge Oliveira, Celso Silva and José Lopes) for their effort and constant support regarding the Sapelos' survey.

A special acknowledgment is also due to Bruno Delfim, currently researching the Iron Age settlements of the PAVT area, for the archaeological feedback regarding this case study.

REFERENCES

[1] Wynn, J. C., "A review of geophysical methods used in archaeology," Geoarchaeology **1**(3), 245–257, John Wiley & Sons, Inc. (1986).

[2] Campana, S., Piro, S., [Seeing the Unseen], CRC Press/ Balkema, LONDON (2009).

[3] Papadopoulos, N. G., Sarris, A., Parkinson, W. A., Gyucha, A., Yerkes, R. W., Duffy, P. R.., Tsourlos, P., "Electrical Resistivity Tomography for the Modelling of Cultural Deposits and Geomophological Landscapes at Neolithic Sites : a Case Study from Southeastern Hungary," Archaeol. Prospect. **21**(February), 169–183 (2014).

[4] Sala, R., Garcia, E.., Tamba, R., "Archaeological Geophysics – From Basics to New Perspectives," [Archaeology, New Approaches in Theory and Techniques] (2000).

[5] Fontes, L.., Alves, M., "O Parque Arqueológico do Vale do Terva. Um Projeto de Paisagem Cultural," [Paisagens Mineiras Antigas na Europa Ocidental. Investigação e Valorização Cultural. Atas do Simpósio Internacional (Boticas, 25-27 Julho de 2014)], L. Fontes, Ed., Câmara Municipal de Boticas, Boticas, 113–142 (2014).

[6] Pereira, B.., Azevedo, J., "Prospeção geofísica e modelação tridimensional do Castro de Sapelos. Relatório Final," Braga (2014).

[7] Schroeder, W., Martin, K., Lorensen, B., [The Visualization Toolkit: An Object-Oriented Approach To 3D Graphics], Third Edit, 520, Pearson Education, Inc. (2003).

[8] Pereira, E.., Rodrigues, J., "Caracterização geológica do NW de Trás-os-Montes (Chaves, Montalegre e Boticas)," [Mineração e Povoamento na Antiguidade no Alto Trás-os-Montes Ocidental], C. M. B. Martins, Ed., Ed. Afrontamento e Rainho & Neves, Lda., Porto, 19–26 (2010).

[9] Ramos, J. M. F., "Recursos minerais na região do rio Terva (concelho de Boticas)," [Exploração mineira aurífera de época romana no Parque Arqueológico do Vale do terva - Da extração ao Paleoambiente], C. M. B. Martins, Ed., SCANGRAPHIC NICOLA PAPA SAG, LDA, Boticas, 19–36 (2014).

[10] Garcia, E. P., Javier, F., Goberna, C., Manuel, J.., Cuñarro, H., "Petroglifos en los Castros Gallegos," Rev. Guimarães **Volume Esp**(II), 793–818 (1999).

[11] Martins, B. M. S. C., "A depressão de Régua-Chaves-Verin. Contributo para a análise do risco de ravinamento.," Universidade de Coimbra (2009).

[12] Parga-Pondal, I. (Dir)., "Carte Géologique du Nord-Ouest de la Péninsule Ibérique (Hercynien et Ante-hercynién) 1 : 500 000," Direcção Geral de Minas e Serviços Geológicos de Portugal (1967).

[13] Pereira, E. (Dir. ., "Carta Geológica de Portugal à escala 1/200 000. Folha 2.," Instituto Nacional de Engenharia, Tecnologia e Inovação, Lisboa (2000).

[14] Geotomo Software, I., "RES2DINV," x32 3.71, Penang (2011).

[15] Loke, M. H., [Tutorial : 2-D and 3-D electrical imaging surveys], 127, Geotomo Software Malaysia (2001).